北京大学学报(自然科学版) 第 51 卷 第 4 期 2015 年 7 月
Acta Scientiarum Naturalium Universitatis Pekinensis, Vol. 51, No. 4 (July 2015)
doi: 10.13209/j.0479-8023.2015.015

Molecular Dynamics Simulation of Tungsten Ablation under Transient Heat Flux

ZHU Yizhou, YAN Sha†, XUE Jianming, HE Shukai, ZHANG Boyao, WANG Yugang

State Key Laboratory of Nuclear Physics and Technology, School of Physics, Peking University, Beijing 100871;
† Corresponding author, E-mail: syan@pku.edu.cn

Abstract The authors adopt molecular dynamics simulations to get a basic physical image of the tungsten ablation phenomenon induced by intense pulsed ions irradiation. A one-dimension heat transfer model is set up and a series of simulations with different pulse energy fluences are applied. Ablation threshold and ablation depth are calculated and compared with thermal dynamic theoretical values. Energy allocation condition of the simulation system are discussed, which depends on whether the pulse energy exceed ablation threshold. Based on the calculation results, the authors drew a preliminary profile of tungsten ablation under a transient high heat flux brought by energetic ions.

Key words tungsten; molecular dynamics; ablation

暂态强热流作用下钨烧蚀过程的分子动力学模拟

朱一舟 颜莎† 薛建明 贺书凯 张博尧 王宇钢

北京大学物理学院核物理与核技术国家重点实验室, 北京 100871; † 通信作者, E-mail: syan@pku.edu.cn

摘要 采用分子动力学方法, 对金属钨在由离子辐照引起的暂态热流下的烧蚀现象进行研究。建立一维热传模型, 通过施加不同能量的热脉冲, 研究钨靶材的热响应。计算烧蚀阈值并与理论值进行比较, 统计分析烧蚀深度与热脉冲能量的关系。研究热脉冲作用过程中能量的转移分配状况, 并对低于和高于烧蚀阈值下的不同能量分布状况进行讨论。从模拟的角度, 建立一个对钨在离子辐照下烧蚀过程的初步的物理图像。

关键词 钨; 分子动力学; 烧蚀
中图分类号 TG156

Metal ablation has been the subject of thorough investigation for many years. On one hand, understanding the picture of metal target response under transient heat flux is a critical and hot topic from fundamental perspective; on the other hand, ablation phenomenon is closely related to many experimental applications.

Recently, tungsten and tungsten-alloy, have drawn much attention in materials science research, since they are viewed as the most promising candidates for divertor armor material in future nuclear fusion devices[1−3]. The main advantage of W is its excellent thermal property: high melting point (3695 K) and good thermal conductivity. Besides, tungsten has low sputtering yield and low tritium inventory, which minimizes the possible effect on the operation of core plasma[3]. However, a critical challenge for tungsten is confronting transient high heat flux, which may exceed the endurance of armor material, resulting in damaging process, including

国家重点基础研究发展计划(2010CB832902)和国际热核聚变实验反应堆(ITER)计划专项(2010GB109004)资助
收稿日期: 2014−04−16; 修回日期: 2014−09−26; 网络出版日期: 2015−04−21

blistering, melting, cracking, sputtering, ablation, etc[4–6]. Divertor armor is an indispensable element in current design of controlled thermonuclear fusion. From both fundamental and applied perspective, it is worthwhile to study the response of tungsten under extreme heat load in detail.

Our attention focuses on the ablation process of tungsten under transient high heat flux induced by energetic ion irradiation. Molecular dynamics (MD) is a powerful approach which helps us understanding physical mechanisms at molecular-level. Since ablation process involves various highly non-equilibrium phenomena, such as explosive phase transition, which cannot be described by conventional heat transfer equation, it is necessary to investigate ablation process from molecular perspective.

A simplified simulation model was set up from fundamental perspective to provide preliminary understanding the occurrence of ablation. Due to the limitation of computation resource, currently we neglected the details of interaction process of ions and target, but focused on the subsequent evolution of irradiated target under a simplified transient heat flux.

1 Computational Model and System

1.1 Computational model

After the energetic ions incidence, their kinetic energy transfers to tungsten atoms rapidly. Once the pulse energy fluence exceeds ablation threshold, atoms near surface will be ablated into vacuum. In most cases, the spot size of incident ions is much larger than the depth affected. Thus, we can have a simplified one-dimensional model, with an inward heat flux in one dimension and periodic boundary conditions in the other two perpendicular dimensions.

The energy deposition only takes place within the range of the incident ions. The profile of energy loss can be calculated by SRIM[7]. To investigate the influence of spatial distribution of energy deposition, we compare the two kinds of heat sources, with stepped and trapezoid (with decaying) shape profile in spatial distribution. The results show that total pulse energy, rather than the shape of heat pulse, is the most critical factor affects the ablation process. To save computation resources, we simplifie the heat source as a uniform shape in a specific “heat deposition region”.

Referring to the ion energy in the plasma scrape-off-layer (< 1 keV), the ion-material interaction region should be within a few nanometers of target surface. We choose 3.17 nm-thick heat deposition region in our simulation.

Tungsten has a relative large atomic mass (183.84 u). So when it is irradiated by light atoms, such as H or He, the dominating kind of energy loss is electronic energy loss rather than nuclear energy loss. Based on this fact, we can use a Langevin thermostat to simulate the irradiation process, in which thermal energy are transferred from a background implicit solvent (in this case, it refers to the electron subsystem) to ion subsystem.

The electron subsystem takes only a few femtoseconds approximately to heat up. However, the lattice system costs more time to absorb the energy. For metal, the electron-phonon coupling time is typically in a magnitude of hundred femtoseconds[8], so the transient thermal process induced by ions should last at least the same period. Therefore, we adopt heat pulse duration of 100 fs.

After loading the pulse, the last step of our simulation is NVE relaxation. The whole system is relaxed with conservative energy. When the pulse fluence is low, the sample might merely expand, but still retain lattice structure. However, once the pulse fluence exceeds ablation threshold, surface atoms will be ablated outward, accompanied by a pressure wave propagating in the remaining bulk. We adopt a timestep of 1 fs and 100000 steps per simulation, a total of 100 ps real time was achieved in this relaxation step.

Finally, we run in house code to do post-process analysis. These results are presented in Section 2.

1.2 System

Our simulations were performed with LAMMPS (large-scale atomic/molecular massively parallel simulator) package[9]. The system we examined was pure tungsten with BCC lattice structure. The lateral x

and *y* dimensions of the system are 18.99 nm × 18.99 nm, while the longitudinal *z* dimension is 15.83 nm. Bulk tungsten lattice consists of 363600 atoms in total.

As discussed above, we are investigating a one-dimension problem, so periodic boundary conditions are applied in the lateral directions. The top surface is set to be free, and the periphery atoms of the bottom surface are frozen at their original position to avoid the remaining lattice being recoiled out of the target frame (when ablation occurs, an intense pressure wave is generated simultaneously in the remaining bulk, causing the recoil of remaining target. The details of pressure wave propagating will be discussed in another paper). Before applying heat load, initial system is equilibrated at 300 K.

Several interaction potentials for tungsten have been developed[10–12] and compared to both experimental and theoretical data[13–14] by other researchers. In our work, we chose the Finnis-Sinclair potential[10]. Because it has a relatively simple form and can well describe thermal and elastic properties of tungsten, including melting point, entropy of melting and vaporization, heat capacity, thermal expansion coefficient and so forth[13].

2 Results and Discussion

Based on above described model, we investigated ablation characteristics of tungsten. A series of stepped inward pulse fluence, ranging from 27.8 J/m^2 to 434.1 J/m^2, is applied in our simulation. In our preliminary research, we mainly investigated the ablation threshold, ablation depth, and energy allocation conditions.

2.1 Ablation threshold

Ablation threshold is directly reflected by the ablated mass loss. The relationship between ablation mass loss and pulse fluence is shown in Fig. 1. When pulse energy reaches around 120 J/m^2, a significant increase in ablated mass loss is observed. Thus we can deduce that the ablation threshold for our system is 120 J/m^2.

To verify this result, we calculated theoretical

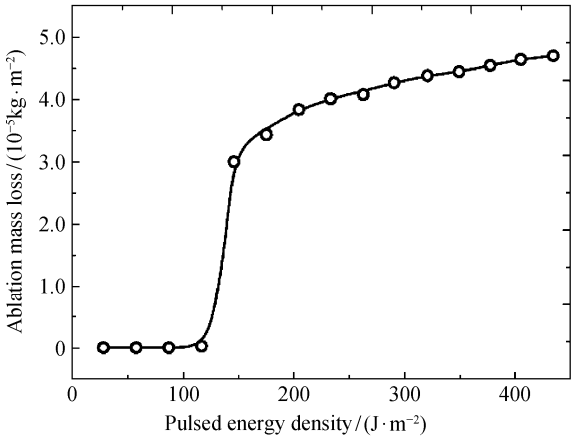

Fig. 1 Mass loss of ablated material verses pulse fluence

threshold fluence using a method similar to one described in Ref. [15]. Given that the theoretical enthalpy of evaporation for tungsten is 86.5 GJ/m^3, we can obtain a theoretical estimation of single-pulse threshold to be 173 J/m^2. Notice that in the theoretical estimation, we are using enthalpy of evaporation, namely, we assume that the ablated material all in gaseous state. Nevertheless, a number of clusters are entrained in the plume, indicating that the potential energy of ablated material remains negative. This probably explains the difference between the two results. With consideration of this factor, our simulation results is in good agreement with the theoretical value.

2.2 Ablation depth

Measurements of the ablation depth can also provide important information about the material response to transient heat load. Fig. 2 shows the dependence of ablation depth on applied pulse fluence. Since fluence is plotted on logarithmic scale, the linearity suggests logarithmic relationship. Thus the logarithmic relationship between ablation depth *d* and pulse fluence *F* can be written as:

$$d = l \cdot \ln\left(\frac{F}{F_{\text{th}}}\right), \tag{1}$$

where F_{th} denotes ablation threshold, and *l* is a fitting parameter. From slope of the line we can deduce *l* equals to 3.35 nm.

Similar logarithmic relationship is observed in

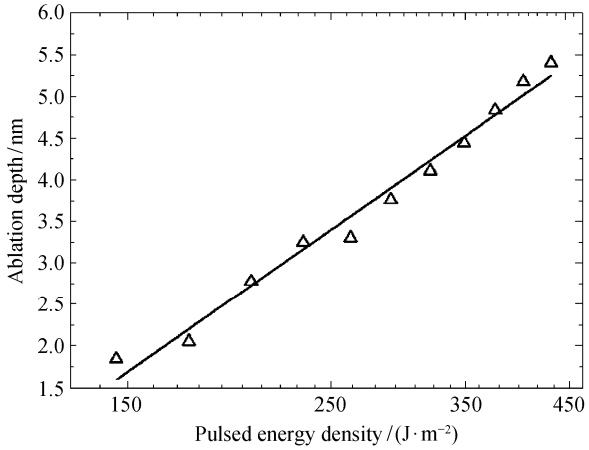

Fig. 2　Ablation depth verses pulse energy fluence

laser ablation experiment for aluminum, copper, silver and tungsten, in which the parameter l refers to the penetration depth or thermal diffusion depth depending on certain conditions[15–16]. We can speculate that l is a parameter associated with the affecting depth of external heat pulse. Specifically in our model, it should be related to the energy deposition range, namely 3.17 nm. Nevertheless, we cannot neglect the fact that laser energy deposition has a different decay profile (exponential) from ion energy deposition. The similarity and difference in ablation depth relationship between different kinds of heat sources call for further investigation.

2.3　Energy allocation conditions

We also paid attention to the energy allocation conditions under heat pulses with different pulse energy. Fig. 3 shows the energy allocation conditions within the initial and final snapshots under different heat pulses. The left bar represents the initial total energy, which consists of only two parts: the initial kinetic energy of tungsten lattice atoms (equilibrated at 300 K) and the external heat pulse energy, while the right bar includes two or three parts depending on whether ablation occurs. Below the ablation threshold, we have only kinetic energy of lattice atoms, and increased potential energy ΔE_p. However, once the pulse energy exceeds the threshold, ablation occurs and we calculate the kinetic energy of ablated atoms and remaining bulk atoms respectively.

From the double bar graph, we can observe that our simulation is in complete accord with energy reservation. What is more, when below the ablation threshold, kinetic energy of lattice atoms and ΔE_p share similar growth rates. This is because that higher temperature leads to both expansion of tungsten lattice and faster random motion speed of lattice atoms. However, after surpassing the threshold, potential energy increase will take a larger part in the energy allocation. This could be explained that these ablated

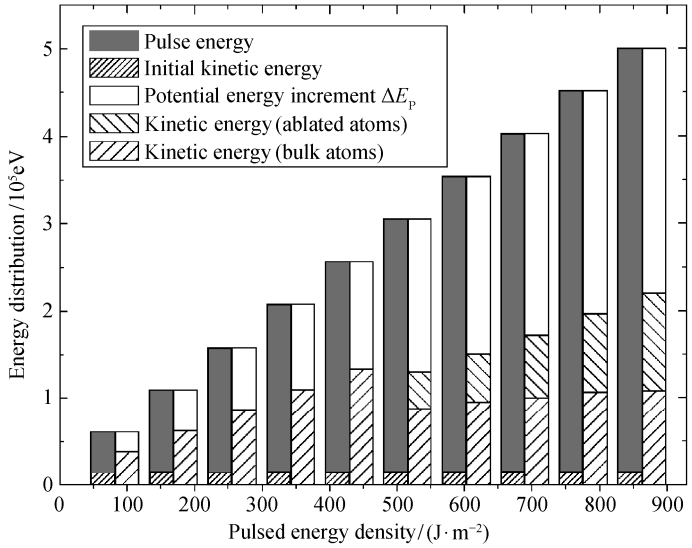

Fig. 3　Energy allocation conditions under heat pulse with different energy

clusters demand much more energy to overcome lattice binding than mere heat expansion.

The double bar graph presents the energy allocation conditions of our simulation system in initial and final stage. The total energy at the initial stage consists of external heat pulse and initial thermal energy of tungsten lattice. While at the final stage, these energy converted to increased potential energy ΔE_p of the entire system, kinetic energy of remaining tungsten lattice atoms, and kinetic energy of ablated atoms (if ablation occurs).

3 Conclusion

Based on our MD simulation in which a simplified one-dimensional heat flux model is adopted, we preliminary outlined some major characters of tungsten ablation under a transient high heat flux induced by intense pulsed ion beam irradiation.

We obtained our estimation of ablation threshold, which is in good agreement with theoretical data. Logarithmic relationship between ablation depth and pulse fluence is found. Moreover, we examined the energy allocation conditions of the system, at both the initial and final snapshots. The results show that occurrence of ablation leads to increasing percentage of external pulse energy that converts to potential energy of the system, which enables atoms to overcome the binding of lattice.

The work we finished here is merely a preliminary approach to understand the outline of ablation process, mainly concerned the target itself. The ablating plume characters, including size and velocity distribution of ablated clusters, will be discussed in another paper. Additionally, pressure wave propagation in the remaining sample target will be investigated in our future research.

References

[1] Davis J W, Barabash V R, Makhankov A, et al. Assessment of tungsten for use in the ITER plasma facing components. J Nucl Mater, 1998, 258: 308–312

[2] Roedig M, Kuehnlein W, Linke J, et al. Investigation of tungsten alloys as plasma facing materials for the ITER divertor. Fusion Eng Des, 2002, 61: 135–140

[3] Federici G, Andrew P, Barabaschi P, et al. Key ITER plasma edge and plasma-material interaction issues. J Nucl Mater, 2003, 313–316: 11–22

[4] Thoma A, Asmussen K, Dux R, et al. Spectroscopic measurements of tungsten erosion in the ASDEX upgrade divertor. Plasma Phys, 1997, 39: 1487–1499

[5] Mayer M, Andrzejczuk M, Dux R, et al. Tungsten erosion and redeposition in the all-tungsten divertor of ASDEX upgrade. Phys Scr, 2009, T138: 014039

[6] Brezinsek S, Kreter A, Philipps V, et al. Tungsten divertor erosion in all metal devices: lessons from the ITER like wall of JET. J Nucl Mater, 2013, 438: S42–S47

[7] Biersack J P, Haggmark L G. A Monte Carlo computer program for the transport of energetic ions in amorphous targets. Nucl Instruments Methods, 1980, 174(1): 257–269

[8] Zhang J, Lang M, Ewing R C, et al. Nanoscale phase transitions under extreme conditions within an ion track. J Mater Res, 2011, 25(7): 1344–1351

[9] Plimpton S. Fast parallel algorithms for short-range molecular dynamics. J Comput Phys, 1995, 117(1): 1–19

[10] Finnis M W, Sinclair J E. A simple empirical N-body potential for transition metals. Philos Mag A, 1984, 50(1): 45–55

[11] Baskes M. Modified embedded-atom potentials for cubic materials and impurities. Phys Rev B, 1992, 46(5): 2727–2742

[12] Dai X D, Kong Y, Li J H, et al. Extended Finnis-Sinclair potential for BCC and FCC metals and alloys. J Phys Condens Matter, 2006, 18(19): 4527–4542

[13] Ryu S, Cai W. Comparison of thermal properties predicted by interatomic potential models. Model Simul Mater Sci Eng, 2008, 16(8): 085005

[14] Liu C M, Chen X R, Xu C, et al. Melting curves and entropy of fusion of body-centered cubic tungsten under pressure. J Appl Phys, 2012, 112(1): 013518

[15] Byskov-Nielsen J, Savolainen J M, Christensen M S, et al. Ultra-short pulse laser ablation of copper, silver and tungsten: experimental data and two-temperature model simulations. Appl Phys A, 2011, 103(2): 447–453

[16] Sonntag S, Paredes C T, Roth J, et al. Molecular dynamics simulations of cluster distribution from femtosecond laser ablation in aluminum. Appl Phys A, 2011, 104(2): 559–565